

Noise correlations of one-dimensional Bose mixtures in optical lattices

Anzi Hu, L. Mathey, Carl J. Williams and Charles W. Clark

Joint Quantum Institute, University of Maryland and National Institute of Standards and Technology, Gaithersburg, MD 20899

We study the noise correlations of one-dimensional binary Bose mixtures, as a probe of their quantum phases. In previous work [23], we found a rich structure of many-body phases in such mixtures, such as paired and counterflow superfluidity. Here we investigate the signature of these phases in the noise correlations of the atomic cloud after time-of-flight expansion, using both Luttinger liquid theory and the time-evolving block decimation (TEBD) method. We find that paired and counterflow superfluidity exhibit distinctive features in the noise spectra. We treat both extended and inhomogeneous systems, and our numerical work shows that the essential physics of the extended systems is present in the trapped-atom systems of current experimental interest. For paired and counterflow superfluid phases, we suggest methods for extracting Luttinger parameters from noise correlation spectroscopy.

I. INTRODUCTION

In recent years, the study of noise correlations has been established as a way of probing ultracold atom systems [1–3]. First proposed in Ref. [4], noise correlation spectroscopy has been discussed as a way of measuring correlation functions of cold atom systems, such as pairing or density order [5–9]. In the experiments reported in Refs. [1–3], a cold atomic gas is first held in a trap, and then released from it by turning off the trapping potential. The noise correlations are measured as the spatial correlations of the density in the fully expanded atomic cloud. If atomic interactions during the expansion can be ignored, one can use the noise correlation measurements to infer momentum space correlations in the initial state. Such an analysis has been used to demonstrate the phase transition between superfluid (SF) and Mott insulator (MI) states [1, 3], as well as the formation of fermionic pairs [2].

The experimental realization of quasi-one dimensional many-body systems with ultra-cold atoms in optical lattices has been reported in Refs. [10–18]. Characteristic features of such systems include fluctuating and competing orders. In contrast to higher dimensional systems which exhibit long-range orders, 1D systems typically display only quasi-orders, that are characterized by the algebraic decay of the correlation function of the order parameter. In Refs. [6, 9], noise correlations were shown to be an effective probe of such orders in 1D Fermi systems, for both one- and two-component systems. Similar studies have been done for 1D bosonic systems, either in the hard-core limit [19] or using Luttinger liquid (LL) theory [5]. In Ref. [5], the signature of condensates and quasi-condensates was discussed in detail.

Noise correlations can also be used to study the phases of binary bosonic mixtures. In such mixtures, two additional orders beyond SF and MI are potentially present, first studied in Ref. [20]. If the inter-species interaction is attractive, bosons of different species can form a paired superfluid (PSF) state. If the interaction is repulsive and the system is confined in a lattice at half-filling, the bosons can form particle-hole pairs, called “anti-pairs”.

Such anti-pairs can then form a counter-flow superfluid (CFSF) state. In addition, a charge density wave order (CDW) can coexist with the three superfluid orders, which is the defining feature of supersolidity. Numerous examples of such order have been given in Refs.[21, 22]. In Ref. [23] we established the phase diagram of a binary mixture exhibiting SF, PSF, CFSF and MI orders, and we showed that each of the superfluid orders can coexist with the CDW order.

We also showed in [23] that because the PSF and CFSF orders are the result of inter-species pairing, they do not provide a signature in the momentum distributions of the individual atomic species. In this paper, we show that noise correlation measurements provide *distinctive* signals of both the PSF and CFSF orders. Ref. [24] shows that noise correlations characteristic of the PSF/CFSF orders can be observed even in a system of only four atoms. Here we calculate the noise correlation spectra from first principles, using the time-evolving block decimation (TEBD) method [25], which is supported by analytical calculations based on LL theory. We make appropriate comparisons between results for homogeneous and trapped systems.

To evaluate the noise correlations, we first assume ballistic expansion and long expansion time and define the noise correlations as the density correlations in momentum space,

$$\mathcal{G}_{aa'}(k, k') = \langle n_{a,k} n_{a',k'} \rangle - \langle n_{a,k} \rangle \langle n_{a',k'} \rangle \quad (1)$$

where a, a' are species indices ($a, a' = 1, 2$), k, k' are momenta, and $n_{a,k}$ and $n_{a',k'}$ are the occupation operators in momentum space. We also consider the derived quantities $C_{aa'}(q)$ and $D_{aa'}(q)$, defined as

$$C_{aa'}(2q) = \int dk \frac{\langle n_a(k+q) n_{a'}(k-q) \rangle}{\langle n_a(k+q) \rangle \langle n_{a'}(k-q) \rangle}, \quad (2)$$

and

$$D_{aa'}(2q) = \int dk \frac{\langle n_a(k+q) n_{a'}(q-k) \rangle}{\langle n_a(k+q) \rangle \langle n_{a'}(q-k) \rangle}. \quad (3)$$

Each of these quantities can capture the main features of the noise correlations for particular types of order and

can be directly measured in experiments [3]. We will present all our results first in the form of $\mathcal{G}_{aa'}(k, k')$ and then use $C_{aa'}(q)$ and $D_{aa'}(q)$ to highlight the key features.

This paper is organized as follows: in Sec. II, we explain our model and the different quasi-orders present in it; in Sec. III, we show our LL results and predict the generic signature of the noise correlations for different orders. In Sec. IV, we present our numerical calculation of noise correlations for both homogeneous and trapped systems. In Sec. V we conclude.

II. NOISE CORRELATIONS AND QUASI-ORDERS

We work in an approximation in which binary Bose mixtures in optical lattices are described by a two-component Bose-Hubbard model [23, 26]. The Hamiltonian for M atoms of each species confined to an optical lattice with N sites is given by

$$H = -t \sum_{a=1,2} \sum_{j=1}^{N-1} (b_{a,j}^\dagger b_{a,j+1} + h.c.) + U_{12} \sum_{j=1}^N n_{1,j} n_{2,j} + \frac{U}{2} \sum_{a=1,2} \sum_{j=1}^N n_{a,j} (n_{a,j} - 1). \quad (4)$$

We denote the different atomic species with the index $a = 1, 2$, and the lattice site with index j . We assume that the two species have the same average filling factor, $\nu = M/N \leq 1$, the same intra-species interaction $U > 0$ and hopping parameter $t > 0$. The inter-species interaction is given by U_{12} . The operators $b_{a,j}^\dagger$ and $b_{a,j}$ are the creation and annihilation operators for atoms of type a and site i and $n_{a,j} = b_{a,j}^\dagger b_{a,j}$ are the number operators.

In Ref. [23], we found that there are four different regimes in the phase diagram (besides the collapsed or phase-separated regime that occurs at large $|U_{12}|$): the superfluid (SF), the paired superfluid (PSF), the counterflow superfluid (CFSF) and the Mott insulator (MI) state. In addition, each of the superfluid orders can co-exist with a charge density wave (CDW) order. The existence of any such order is determined from the asymptotic behavior of the correlation functions of the corresponding order parameters. Specifically, the single-species superfluid (SF) has the order parameter $b_a(x)$ ($a = 1, 2$) and its corresponding correlation function $G(x) = \langle b_a^\dagger(x) b_a(0) \rangle$; the paired superfluid (PSF) has the order parameter $b_1(x) b_2(x)$ and its corresponding correlation function $R_S(x) = \langle b_1^\dagger(x) b_2^\dagger(x) b_1(0) b_2(0) \rangle$; the counter-flow superfluid (CFSF) has the order parameter $b_1(x) b_2^\dagger(x)$ and its corresponding correlation function $R_A(x) = \langle b_1^\dagger(x) b_2(x) b_1(0) b_2^\dagger(0) \rangle$. The CDW order parameter is $n_a(x)$ ($a = 1, 2$) and the corresponding correlation function $R_{n,a}(x) = \langle n_a(x) n_a(0) \rangle$. The asymptotic behavior of the correlation functions at large x is listed in

	$R_S(x)$	$R_A(x)$	$G(x)$	$R_{n,a}(x)$
MI	E	E	E	A
SF	A	A	A	A
CFSF	E	A	E	A
PSF	A	E	E	A
CDW	A or E	A or E	A or E	A ($\alpha < 2$)

Table I: Definitions of MI, SF, CFSF and PSF orders in terms of the large x behavior of the correlation functions $R_S(x)$, $R_A(x)$, and $G(x)$, $R_{n,a}(x)$. A: algebraic decay of the form $x^{-\alpha}$; E: exponential decay of the form $e^{-\beta x}$. A correlation function is said to exhibit quasi-order when it is subject to algebraic decay with $\alpha < 2$. In this system, the algebraic decay for R_S , R_A and G always has $\alpha < 2$, while $R_{n,a}$ can have $\alpha \geq 2$. CDW quasi-order exists only when $R_{n,a}$ is described by $\alpha < 2$.

Table. I for the different phases.

We calculate the noise correlations from the four-point correlation function:

$$\mathcal{G}_{aa'}(k, k') = \sum_{j_1, j_2, j_3, j_4=1}^N \mathcal{L}_{aa'}(j_1, j_2, j_3, j_4) e^{i[kj_{12} + k'j_{34}]} - \langle n_a(k) \rangle \langle n_{a'}(k') \rangle, \quad (5)$$

where $j_{12} \equiv j_1 - j_2$, $j_{34} \equiv j_3 - j_4$ and $\mathcal{L}_{aa'}$ is the four-point correlation function,

$$\mathcal{L}_{aa'}(j_1, j_2, j_3, j_4) = \langle b_{a,j_1}^\dagger b_{a,j_2} b_{a',j_3}^\dagger b_{a',j_4} \rangle. \quad (6)$$

It is easy to see that the correlation functions R_S , R_A and $R_{n,a}$ are the special cases of $\mathcal{L}_{aa'}$,

$$\begin{aligned} \mathcal{L}_{12}(j_1, j_2, j_1, j_2) &= R_S(j_1, j_2), \\ \mathcal{L}_{12}(j_1, j_2, j_2, j_1) &= R_A(j_1, j_2), \\ \mathcal{L}_{aa}(j_1, j_2, j_2, j_1) &= R_{n,a}(j_1, j_2) + n_{a,j_1}. \end{aligned} \quad (7)$$

The noise correlation \mathcal{G}_{12} , therefore, contains the Fourier transform of R_S and R_A ,

$$g_S(k, k') = \sum_{j_1, j_2} R_S(j_1, j_2) e^{i(k+k')(j_1-j_2)} \quad (8)$$

and

$$g_A(k, k') = \sum_{j_1, j_2} R_A(j_1, j_2) e^{i(k-k')(j_1-j_2)} \quad (9)$$

and \mathcal{G}_{aa} contains the Fourier transform of $R_{n,a}$,

$$g_{n,a} = \sum_{j_1, j_2} R_{n,a}(j_1, j_2) e^{i(k-k')(j_1-j_2)}. \quad (10)$$

If $R_S(j_1, j_2)$ decays as $|j_1 - j_2|^{-1/K_S}$, we find that g_S scales as $|k + k'|^{-1/K_S}$. Similarly, if R_A decays as $|j_1 - j_2|^{-1/K_A}$, g_A scales as $|k - k'|^{-1/K_A}$. For the PSF

phase, we find that $g_s(k, k')$ is the dominant term of $\mathcal{G}_{12}(k, k')$ with a strong peak around $k = -k'$. This peak is the signal of the PSF order. Similarly, for the CFSF phase, we find that the function $g_A(k, k')$ becomes dominant around $k = k'$ in $\mathcal{G}_{12}(k, k')$. The peak around $k = k'$ is the signal of the CFSF order. These remarks are made to give the reader an intuitive interpretation of the relationship between the noise correlations and the long-range orders. In the following section, we will explain the calculation of the noise correlations via LL theory and show that the features mentioned above are indeed reflected in the LL calculation results.

III. LUTTINGER LIQUID APPROACH

In this section we determine the generic behavior of the noise correlations using a Luttinger liquid approach. This formalism has been applied to one-dimensional Fermi systems in Ref. [6], and additionally to single-species bosonic systems in Ref. [5], where a detailed description of these calculations was given. Here, we use an analogous derivation for the case of a bosonic mixture. We outline key steps of the derivation, but refer the reader to Ref. [5] for a detailed description of the method.

As described in Ref. [23], we switch to a continuum description, in which the single particle operators are given by $b_a(x)$. We then use a bosonization identity [27, 28]

$$b_a(x) = [n + \Pi_a(x)]^{1/2} \sum_m e^{2im\Theta_a(x)} e^{i\phi_a(x)}, \quad (11)$$

where n is the real space density, related to the filling factor by $n = \nu/a_L$, where a_L is the lattice constant, and m is an integer summation index. For future reference, we note that the Fermi wavevector of an equivalent system of fermions, k_F , is given by $k_F = \pi n$. Although this paper describes a bosonic system, we find that the Fermi wavevector occurs naturally in a number of contexts. For example, Θ_a is given by $\Theta_a(x) = k_F x + \theta_a(x)$, where $\theta_a(x) = \pi \int^x dy \Pi_a(y)$. Π_a describes the low-momentum density fluctuations of species a and $\phi_a(x)$ is the phase field of species a .

We calculate the noise correlations at the Gaussian fixed point, corresponding to the SF phase. Here, the system separates into symmetric and anti-symmetric degrees of freedom, defined as $\theta_{S,A} = (\theta_1 \pm \theta_2)/\sqrt{2}$ and $\phi_{S,A} = (\phi_1 \pm \phi_2)/\sqrt{2}$. The action can be written either in terms of the phase fields

$$S = \sum_{j=S,A} \int d^2 r_j \left[\frac{K_j}{2\pi} [(\partial_{v_j\tau} \phi_j)^2 + (\partial_x \phi_j)^2] \right], \quad (12)$$

or in terms of the fields $\theta_{S,A}$

$$S = \sum_{j=S,A} \int d^2 r_j \left[\frac{1}{2\pi K_j} [(\partial_{v_j\tau} \theta_j)^2 + (\partial_x \theta_j)^2] \right]. \quad (13)$$

The velocities $v_{S,A}$ are the phonon velocities of the symmetric/anti-symmetric modes, and $\mathbf{r}_{S,A} = (v_{S,A}\tau, x)$.

The parameters $K_{S,A}$ are the Luttinger parameters of the symmetric/anti-symmetric sector. To calculate the noise correlations away from the SF regime, we take the limits $K_{S,A} \rightarrow 0$ to describe the phases in which either or both $R_{S/A}$ have short-ranged correlations (exponential decay). This approximation corresponds to the limit that the length scale of the exponential decay is much smaller than any other length scale of the system. Our calculation could be extended in a straightforward way to include a finite decay length of the exponential decay.

We start out by calculating $\langle n_{a,k} \rangle$ for small momentum $k \approx 0$, for which the Bose operators are given by $b_a \sim \sqrt{n} e^{i\phi_a}$. For $\langle n_{a,k} \rangle$ we find:

$$\langle n_{a,k} \rangle \sim n \int dx_{12} e^{ikx_{12}} e^{-\frac{1}{2} \langle (\phi_a(2) - \phi_a(1))^2 \rangle}, \quad (14)$$

where $\phi_a(1)$ refers to $\phi_a(x_1)$, and similarly for $\phi_a(2)$, and $x_{12} = x_1 - x_2$. The correlation function $\langle (\phi_a(2) - \phi_a(1))^2 \rangle$ can be rewritten in terms of correlation functions for $\phi_{S,A}$. Using the Gaussian action above, we find

$$\langle (\phi_{S/A}(2) - \phi_{S/A}(1))^2 \rangle = \frac{1}{2K_{S/A}} \log \frac{r_0^2 + x_{12}^2}{r_0^2}, \quad (15)$$

where r_0 is a short-range cut-off. With that we find

$$\langle n_k \rangle \sim n \int dx_{12} e^{ikx_{12}} \mathcal{F}(x_{12}), \quad (16)$$

where

$$\mathcal{F}(x) = \left(\frac{r_0^2}{r_0^2 + x^2} \right)^g. \quad (17)$$

The exponent g is given by $g = 1/8K_S + 1/8K_A$. Next we evaluate the expectation value $\langle n_k n_{k'} \rangle$ along the same lines. We obtain:

$$\langle n_{1,k} n_{1,k'} \rangle \sim n^2 \int e^{ikx_{12} + ik'x_{34}} \mathcal{F}(x_{12}) \mathcal{F}(x_{34}) \mathcal{A} \quad (18)$$

where

$$\mathcal{A} = \left(\frac{(r_0^2 + x_{14}^2)(r_0^2 + x_{23}^2)}{(r_0^2 + x_{13}^2)(r_0^2 + x_{24}^2)} \right)^h, \quad (19)$$

and Eq. 18 is a volume integral over the spatial variables x_{12}, x_{23}, x_{34} . The exponent h is given by $h = -1/8K_S - 1/8K_A$. We combine these expressions to get the correlation function $\mathcal{G}_{11}(k, k')$:

$$\begin{aligned} \mathcal{G}_{11}(k, k') \\ \sim n^2 \int e^{ikx_{12} + ik'x_{34}} \mathcal{F}(x_{12}) \mathcal{F}(x_{34}) (\mathcal{A} - 1). \end{aligned} \quad (20)$$

For $\mathcal{G}_{12}(k, k')$ we proceed analogously, and find $h = -1/8K_S + 1/8K_A$. For the finite-size systems that we treat here, we evaluate these integrals numerically, by choosing a finite length L of the system, and by replacing each spatial variable x by $(L/2\pi) \sin(2\pi x/L)$ (see Ref.

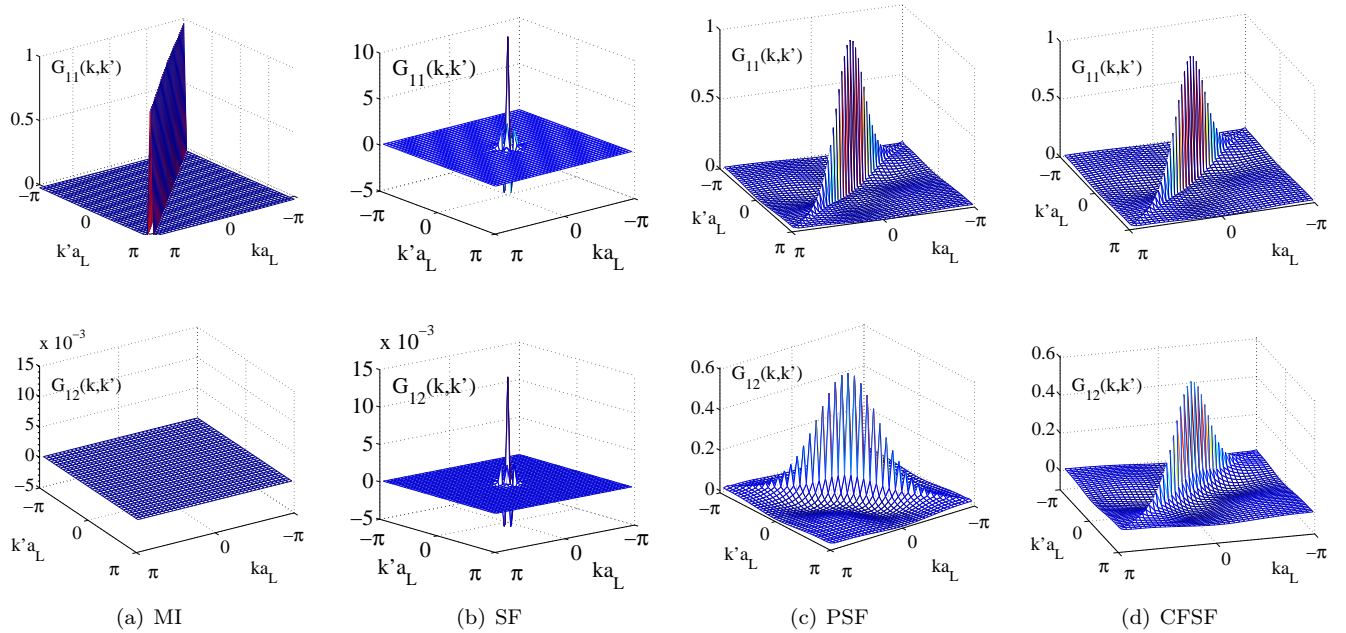


Figure 1: Noise correlations in different phases, derived from Luttinger liquid theory. In the MI state (column (a)), δ -function like correlations along $k = k'$ in $\mathcal{G}_{11}(k, k')$ are visible, whereas \mathcal{G}_{12} nearly vanishes. In the SF state (column (b)), with Luttinger parameters $K_A = 1.03$ and $K_S = 0.96$, we find various contributions in \mathcal{G}_{11} , especially δ -function along $k = k'$. In Fig. 2, we show the contour plots for \mathcal{G}_{11} and \mathcal{G}_{12} for the same state, where we can see the negative correlations at $k = 0$ and $k' = 0$, as well as pairing correlation along $k = -k'$, which is similar to the single-species result in Ref. [5]. \mathcal{G}_{12} shows similar features, but the bunching contribution is an algebraic peak, rather than a δ -function. In (c) we show an example for the PSF phase, with $K_A = 0.01$ and $K_S \simeq 1.3$, in (d) an example for the CFSF phase, with $K_S = 0.01$ and $K_A \simeq 1.2$. In the PSF state, the inter-species correlation $\mathcal{G}_{12}(k, k')$ has strong correlations along $k = -k'$, a reflection of pairing. In the CFSF state, the peak is formed along $k = k'$ direction, an indication of the anti-pairing (particle-hole) formation in the CFSF state.

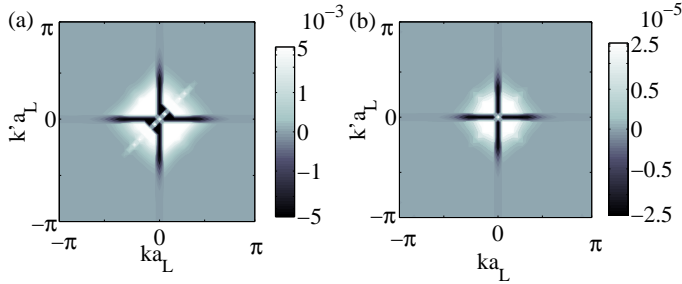


Figure 2: Noise correlations, $\mathcal{G}_{11}(k, k')$ (a) and $\mathcal{G}_{12}(k, k')$ (b), in the SF state. The data used here are the same as those used in Fig. 1 (b). We create the non-linear gray scales by plotting functions $\tanh(500\mathcal{G}_{11})$ (a) and $\tanh(10^5\mathcal{G}_{12})$ (b), in order to magnify the details around $k = k' = 0$. The labels of the color-bar reflect the values of $\mathcal{G}_{11}(k, k')$ and $\mathcal{G}_{12}(k, k')$. In these plots, we can clearly see the negative correlations between the quasi-condensate ($k = 0$ and $k' = 0$) and the higher momentum states at the quantum depletion, as well as the anti-pairing correlation along $k = k'$ and the pairing correlation along $k = -k'$.

[29]). To compare with the TEBD calculations of a homogeneous system in the next section, we choose the values of the Luttinger parameters, K_A and K_S to those ob-

tained from the TEBD calculations and they are listed in Table. II.

In Fig. 1 (b) and 2, we show an example for the SF regime. In the upper panel of Fig. 1 (b), we show $\mathcal{G}_{11}(k, k')$, in the lower panel $\mathcal{G}_{12}(k, k')$. The Luttinger parameters are $K_A = 1.03$ and $K_S = 0.96$. The ratio L/r_0 was chosen as $L/r_0 = 20$, corresponding to the particle number of each species in the numerical example. The shape of $\mathcal{G}_{11}(k, k')$ is the same as the noise correlation function for a single bosonic SF, which was discussed in Ref. [5]. It has the characteristic features of a superfluid: positive correlations along $k = -k'$, which indicates pairing correlations; negative correlations for the axes $k = 0$ and $k' = 0$, indicating the negative correlations between the quasi-condensate and the higher momenta due to pair fluctuations; and bunching correlations along $k = k'$. For $\mathcal{G}_{12}(k, k')$ we find qualitatively a similar shape, with the main difference, that the bunching along $k = k'$ does not have a δ -function contribution, but only algebraic terms. We note that for a system of two non-interacting species, i.e. for $U_{12} = 0$, $K_S = K_A$, and \mathcal{G}_{12} vanishes.

In Figs. 1 (c) and (d) we show the noise correlations for the PSF and the CFSF phase, respectively. For the PSF example, the Luttinger parameters are $K_S = 1.3$

and $K_A = 0.01$. For L/r_0 we again pick $L/r_0 = 20$. For the CFSF phase, the parameters are $K_A = 1.2$ and $K_S = 0.01$. In the PSF regime, we find a strong pairing signature in \mathcal{G}_{12} , similar to the pairing signature in Fermi mixtures [5, 6]. In the CFSF example, an strong anti-pairing signature is found in \mathcal{G}_{12} .

We can obtain the functional form of these signatures in the limit $L \rightarrow \infty$, by applying similar arguments to what has been given in Ref. [5]. In the PSF region, We rewrite the noise correlation integral in terms of $z = (x_{12} - x_{34})/2$, $h_+ = (x_{14} + x_{23})/2$ and $h_- = (x_{14} - x_{23})/2$. We then note that for \mathcal{G}_{12} and for $K_A \rightarrow 0$, the exponent $h = -1/8K_S + 1/8K_A$ diverges. This enforces the integrand to be negligible away from z , $h_+ \approx 0$. Thus the integral evaluates to

$$\mathcal{G}_{12} \sim |k + k'|^{-1/K_S}. \quad (21)$$

This is the shape that would be approached in an infinite system by the noise correlations shown in Fig. 1 (c), lower panel. The deviation from the pure power law is due to the finite size of the system. With similar arguments one can show that in the CFSF regime the inter-species noise correlation approaches

$$\mathcal{G}_{12} \sim |k - k'|^{-1/K_A}, \quad (22)$$

for $L \rightarrow \infty$. Again, the deviation from a pure power law is due to the finite size of the system. Furthermore, one can show that for both PSF and CFSF orders, $\mathcal{G}_{11}(k, k')$ approaches $\delta(k - k')$, in the limit of infinite size. Equations 21 and 22 show that there is a simple relationship between \mathcal{G}_{12} and K_S in the PSF regime and \mathcal{G}_{12} and K_A in the CFSF regime. This suggests that a careful measurement of \mathcal{G}_{12} can be used to extract the value of the Luttinger parameters appropriate to the system. This is further confirmed by our numerical calculations for a trapped system, where we show that the algebraic relationship described by Eqs. 21 and 22 remains valid in the presence of a harmonic trap. We discuss prospects for experimental determination of Luttinger parameters in Sec. IV C.

The MI result in Fig. 1 (a) is obtained by setting both K_A and K_S to 0.01. In this case, the ground state closely approximates a simple product of MI states of each species. Thus, \mathcal{G}_{11} approaches a δ -function, whereas \mathcal{G}_{12} nearly vanishes.

Next we calculate the noise correlations for the case $k \approx 0$ and $k' \approx 2k_F$, where k_F is the Fermi wavevector defined above. Essentially the same calculation can be done for $k' \approx -2k_F$, and $k' \approx 0$ and $k \approx \pm 2k_F$. $n_{a,k}$ is still given by the expression (16), but $n_{a,k'}$ now needs to be calculated with the operator representation $b(x) = \sqrt{n} \exp(2i\Theta(x)) \exp(i\phi(x))$. With that we find

$$\langle n_{q'+2k_F} \rangle \sim n \int dx_{12} e^{iq'x_{12}} \mathcal{F}'(x_{12}), \quad (23)$$

where $\mathcal{F}'(x_{12})$ has the same form as before but with an exponent $g' = 1/8K_S + 1/8K_A + (K_S + K_A)/2$. The noise correlations take the form

$$\mathcal{G}_{11}(k, q') \sim n^2 \int e^{ikx_{12} + iq'x_{34}} \mathcal{F}(x_{12}) \mathcal{F}'(x_{34}) (\mathcal{A} - 1). \quad (24)$$

We therefore note that around the points $k \approx 0$ and $k' \approx \pm 2k_F$, and $k \approx \pm 2k_F$ and $k' \approx 0$ the integrand is multiplied by a contribution that is of the form of the integrand of the static structure factor

$$S(q) \sim \int e^{iqx_{12}} \left(\frac{r_0^2}{r_0^2 + x_{12}^2} \right)^{(K_S + K_A)/2}, \quad (25)$$

which can create cusps in the noise correlation when the system is in the CDW regime. These cusps are found in our numerical calculations and are discussed in the next section.

IV. NUMERICAL CALCULATION

The calculation of noise correlations is based on the ground state generated by the time-evolving block decimation method (TEBD). This method has been used to generate the ground state of many 1D models [25]. In this method, the Hilbert space \mathbf{H} is decomposed as

$$\mathbf{H} = \otimes_{l=1}^N \mathbf{H}_l. \quad (26)$$

Here, l refers to the l th lattice site, N is the number of sites, and \mathbf{H}_l is the local Hilbert space at site l with local dimension d , independent of l . Any state $|\Psi\rangle$ in \mathbf{H} is represented as

$$|\Psi\rangle = \sum_{j_1, j_2, \dots, j_M=1}^d c_{j_1, j_2, \dots, j_M} |j_1\rangle |j_2\rangle \cdots |j_M\rangle, \quad (27)$$

where

$$c_{j_1, j_2, \dots, j_M} = \sum_{\alpha_1=1}^{\chi} \sum_{\alpha_2=1}^{\chi} \cdots \sum_{\alpha_{M-1}=1}^{\chi} \lambda_{\alpha_1}^{[1]} \Gamma_{\alpha_1 \alpha_2}^{[1] j_1} \lambda_{\alpha_2}^{[2]} \Gamma_{\alpha_2 \alpha_3}^{[2] j_2} \lambda_{\alpha_3}^{[3]} \cdots \times \lambda_{\alpha_{M-1}}^{[M-1]} \Gamma_{\alpha_{M-1} \alpha_M}^{[M-1] j_{M-1}} \lambda_{\alpha_M}^{[M]} \Gamma_{\alpha_{M-1} \alpha_M}^{[M] j_M} \lambda_{\alpha_{M+1}}^{[M+1]} \quad (28)$$

The variables $\lambda_{\alpha_l}^{[l]}$ and χ_l are the Schmidt coefficients and rank of the Schmidt decomposition of $|\Psi\rangle$ at site l and $\Gamma^{[l]}$ is a rank-three tensor. Further detail on this method is provided in the appendix of the previous publication [23]. Here, we limit ourselves to stating values of parameters and particular methods of calculation. In this work, we set the Schmidt rank $\chi = 100$ and the local dimension $d = 5$. We use imaginary-time propagation to generate the ground state. After obtaining the ground state, we calculate the correlation functions, R_A , R_S , $R_{n,a}$ and G , and determine the quasi-long range order present in the system based on the relationship shown in Table. I. Furthermore, we can extract the value of the Luttinger

Parameter setting	Order	Luttinger Parameters
(a) $U_{12}/U = 0.01, \nu = 1$	Mott Insulator (MI)	$K_A = K_S = 0$
(b) $U_{12}/U = 0.01, \nu = 0.5$	Superfluid (SF)	$K_A \simeq 1.03, K_S \simeq 0.96$
(c) $U_{12}/U = -0.11, \nu = 0.5$	Paired Superfluid (PSF)	$K_A = 0, K_S \simeq 1.3$
(d) $U_{12}/U = 0.11, \nu = 0.5$	Counterflow Superfluid with (CFSF)	$K_A \simeq 1.2, K_S = 0$
(e) $U_{12}/U = 0.26, \nu = 0.2$	Superfluid with charge density wave (SF/CDW)	$K_A \simeq 1.4, K_S \simeq 0.57$

Table II: The parameters used in the numerical examples and the Luttinger parameters extracted from the algebraic fit of correlation functions, R_A and R_S . The Luttinger parameters are set to zero when the correlations decay exponentially. The hopping parameter t is $0.02U$ for all cases. The parameters are chosen to represent different orders that can exist in this system.

parameters, K_A and K_S , from the numerically calculated correlation functions [23]. We use these parameters in a LL calculation to compare the numerical and the analytical results.

The main challenge of determining the noise correlation functions is the high computational cost of calculating the four-point function, $\mathcal{L}_{aa'}(j_1, j_2, j_3, j_4)$ (Eq. 6), which is estimated to scale as $\chi^3 d^3 N^4$. For the system sizes used in this paper, we use parallel computing algorithms to speed up the calculation by parallelization the computation of $\mathcal{L}_{aa'}$ along the indices j_i .

A. Homogeneous system

In this section we discuss the numerical results for noise correlations of a homogeneous system of 40 lattice sites, subject to the hard-wall or “open” boundary condition, in which the wave function is required to vanish on the fictitious sites of index 0 and $N + 1$ implied by Eq. 4. We consider five parameter sets listed in Table II, representing different regimes of the phase diagram of 1D Bose mixtures.

Superfluid and Mott insulator

For the Hamiltonian of Eq. 4, in the non-interacting case, $U_{12} = 0$, SF and MI are the only two possible orders. In the interacting case, SF and MI orders are still encountered, when the inter-species interaction is weak. For the Hamiltonian of Eq. 4 with $t \ll U$, the MI state exists for any $|U_{12}| \lesssim U$, until the occurrence of collapse ($U_{12} \lesssim -U$) or phase separation ($U_{12} \gtrsim U$). The SF state however exists only when $|U_{12}| \ll U$. In either of SF or MI phases, the quasi-order is formed in each individual species and the cross-species correlation is weak.

For the MI state (Fig. 3 (a)) we find that $\mathcal{G}_{11}(k', k)$ shows strong correlations along the direction $k' = k$, in agreement with the LL theory result shown in Fig. 1 (a). We also find that the correlations along $k' = k$ are not uniform and that the peak along $k' = k$ resembles a Lorentzian distribution in k imposed upon a constant. This Lorentzian is due to the characteristic scale of the correlation functions. This contribution was ignored in

the before-mentioned approximation in the LL calculation, but could be included in a straightforward manner. The cross-species noise correlation, $\mathcal{G}_{12}(k, k')$, on the other hand, is essentially zero, indicating the absence of cross-species correlations in the MI state. For the SF state (Fig. 3 (b) and Fig. 4), we consider the case where there is weak repulsion between the two species (Table II (2)). The Luttinger parameters are $K_A = 1.03$ and $K_S \simeq 0.96$, which were extracted from the correlation functions R_S and R_A by numerical fitting. From the upper panel in 3 (b), we see that \mathcal{G}_{11} has the characteristic features of a quasi-condensate [5]: the positive correlations along $k = -k'$, which indicate pairing; the negative correlations between $k = 0$ and finite k' , as well as between $k' = 0$ and finite k ; and a δ -function like correlation along $k = k'$, corresponding to bosonic bunching. The lower panel in Fig. 3 (b), we see \mathcal{G}_{12} , which shows similar features, except for the δ -function along $k = k'$, which is “softened” into a power-law divergence and a slight negative value at $k = k' = 0$. For a system of two non-interacting superfluids, i.e. $U_{12} = 0$, we have $K_S = K_A$, and $\mathcal{G}_{12} = 0$.

Paired superfluid and counter-flow superfluid

We now discuss the noise correlations of the PSF and CFSF states. The noise correlation $\mathcal{G}_{12}(k, k')$ is particularly important for these two phases, because it can verify the existence of PSF and CFSF orders. Unlike SF and MI states, PSF and CFSF states are characterized by order parameters that contain both species and therefore cannot be reflected in any single-species observables, such as the single-particle Green’s function, $G_a(x)$ or the single-particle momentum distribution [23]. The noise correlation function $\mathcal{G}_{12}(k, k')$ measures the correlations between the momentum occupancies of the two species, and thus provides a direct probe of these orders. We have shown in the previous section, that the peak along $k = -k'$ in $\mathcal{G}_{12}(k, k')$ indicates the PSF order and that along $k = k'$ indicates the CFSF order. These features are verified in our numerical calculation of \mathcal{G}_{12} from the ground state.

In Fig. 3 (c), we show the noise correlations in the PSF state. The parameters are listed in (c) of Tab. II.

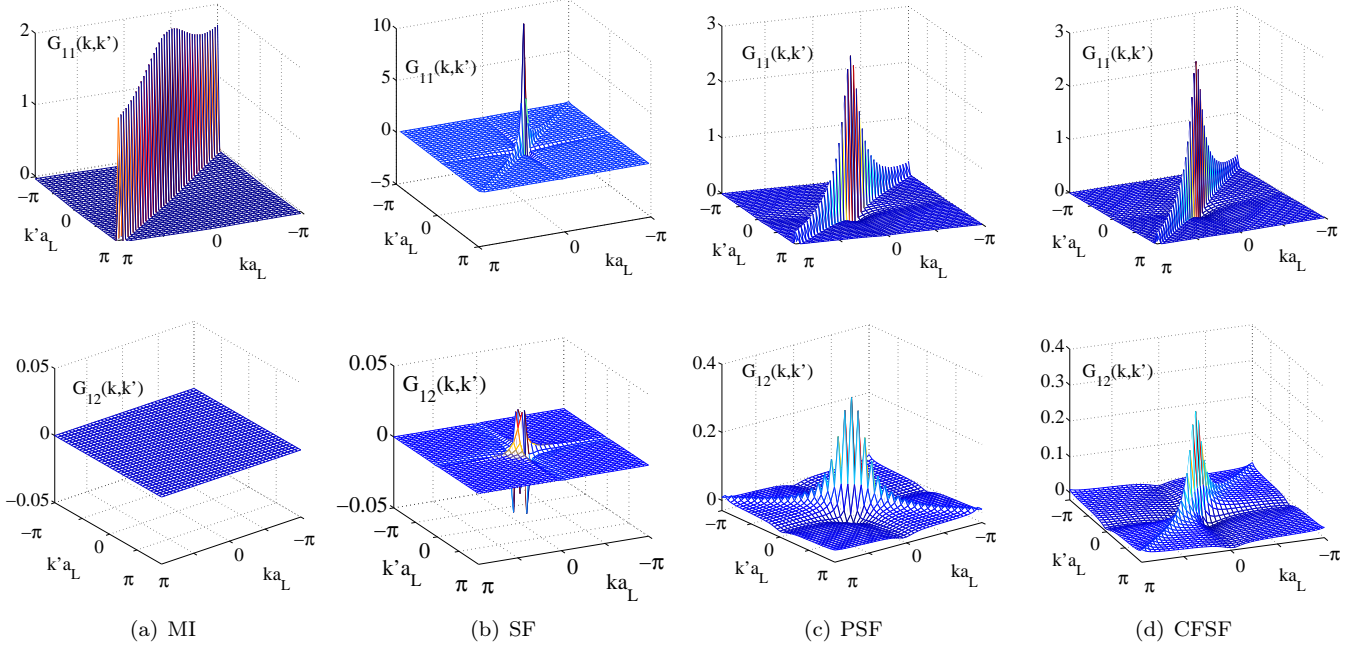


Figure 3: Noise correlations for a homogeneous system of 40 lattice sites, calculated with the TEBD method. The frames (a) – (d) correspond to the examples (a) – (d) in Table II. In (a), we show the noise correlations of a MI state. In the plot of $\mathcal{G}_{11}(k, k')$, there is a strong correlation along the direction $k = k'$, whereas the noise correlation function $\mathcal{G}_{12}(k, k')$ essentially vanishes. In (b), we show the noise correlations of a SF state. Here, we can see the peak around $k = k'$ corresponding to the δ -function bunching peak predicted by LL theory (see also Fig. 1 (b)). For \mathcal{G}_{12} , we find negative value at $k = k' = 0$, which is different from the LL result (Fig. 1 (b)). Other structures predicted by LL theory can be seen in Fig. 4, where \mathcal{G}_{12} and \mathcal{G}_{11} are plotted in a non-linear color scale to magnify the structures around $k = k' = 0$. In (c) and (d), we show the noise correlations of the PSF and CFSF state, respectively. In the PSF state (c), the inter-species correlation $\mathcal{G}_{12}(k, k')$ has strong correlations along $k = -k'$, a consequence of pairing (see also Fig. 1 (c)). In the CFSF state (d), the peak is formed along the direction $k = k'$, an indication of anti-pairing in the CFSF state (see also Fig. 1).

The existence of PSF order is - as usual - determined by the behavior of the $R_S(x)$ and $R_A(x)$. $R_A(x)$ decays exponentially and $R_S(x)$ algebraically with Luttinger parameter $K_S \simeq 1.3$. For the noise correlation function $\mathcal{G}_{12}(k, k')$, we find that a peak is formed along $k = -k'$, which is a consequence of the pairing correlations. In Fig. 3 (d), we show our numerical results for the CFSF example (d) in Table II. Based on the behavior of the $R_S(x)$ and $R_A(x)$ we verify that the system is in a CFSF state with $K_A \simeq 1.2$, and an exponentially decaying $R_S(x)$. For \mathcal{G}_{12} we find that a peak is formed along the diagonal direction, as a result of correlations of anti-pairs ($b_1 b_2^\dagger$). These findings are consistent with the predictions of LL theory (see Fig. 1). We note that $\mathcal{G}_{12}(k, k')$ is enhanced in magnitude in the PSF and the CFSF phase compared to the MI and the SF phase, with a strongly altered functional form.

Charge density wave

In certain parameter regimes of the phase diagram, charge density wave (CDW) order can coexist with each of the three superfluid orders, SF, PSF and CFSF. In

Sect. III, we use LL theory to show that CDW order can be reflected in the function \mathcal{G}_{11} and that the behavior of \mathcal{G}_{11} around $k = k' \pm 2k_F$ resembles the structure factor $S(k)$. The reason for the resemblance can be understood in a simple way, by recalling the definition of the structure factor

$$S(k) = \frac{1}{N} \sum_{j_1, j_2} e^{-ik(j_1 - j_2)} (\langle n_{j_1} n_{j_2} \rangle - \langle n_{j_1} \rangle \langle n_{j_2} \rangle). \quad (29)$$

As mentioned in Sect. II the density correlation function is "contained" in the noise correlations and the term ,

$$\sum_{j_1, j_2=1}^N \langle b_{1, j_1}^\dagger b_{1, j_2} b_{1, j_2}^\dagger b_{1, j_1} \rangle e^{i[k(j_1 - j_2) + k'(j_2 - j_1)]},$$

is part of the full sum that needs to be taken for \mathcal{G}_{11} . This term can also be written as a function of the density operator, $n_j = b_j^\dagger b_j$, as

$$\sum_{j_1, j_2=1}^N \langle n_{j_1} n_{j_2} \rangle e^{-i(k' - k)(j_1 - j_2)} + \delta(k - k') \langle n_{j_1} \rangle e^{-i(k' - k)j_1}$$

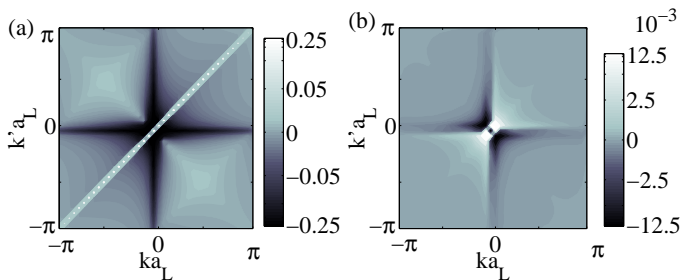


Figure 4: Noise correlations, $\mathcal{G}_{11}(k, k')$ (a) and $\mathcal{G}_{12}(k, k')$ (b), in the SF state of a homogeneous system. The values of $\mathcal{G}_{11}(k, k')$ and $\mathcal{G}_{12}(k, k')$ are exactly the same as in Fig. 3 (b). We create non-linear gray scales by plotting $\tanh(10\mathcal{G}_{11})$ and $\tanh(200\mathcal{G}_{12})$ in linear scales. The labels of the color-bar reflects the values of $\mathcal{G}_{11}(k, k')$ and $\mathcal{G}_{12}(k, k')$. The features around $k = k' = 0$ are magnified as a result of the non-linear scale. In (a), we find the features predicted by LL calculations (2 (a)). In addition, we can see a weak correlation at around $k = k' \pm 2k_F$, where $k_F = \nu \times \pi/a_L = 0.5\pi/a_L$. This is where a strong correlation (cusps) will develop if CDW order is present. This feature can also be shown in LL calculations at around $k \approx 0$ and $k' \approx 2k_F$ (Eq. 24). In (b), we find that the structures along $k = k'$ is similar with the ones in LL calculations, however, the structures along $k = -k'$ is negative, different from the LL predictions (see also Fig. 2). The difference may be understood as a result of different boundary conditions used for the finite-size calculations: the numerical calculations use a “hard-wall” boundary condition, whereas the LL calculations assume a periodic boundary condition.

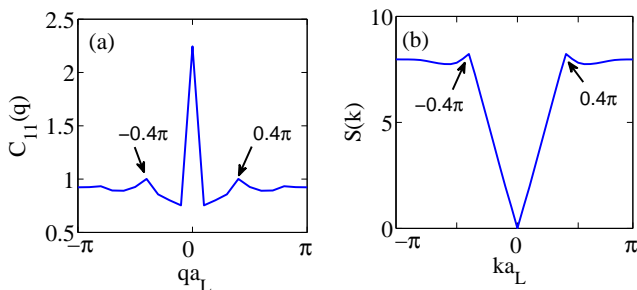


Figure 5: Left : The correlation function $C_{11}(q)$, as defined in Eq. 2; right: the structure factor $S(k)$ for a quasi-supersolid state. The parameters are given in example (5) of Table. II. The Luttinger parameters are $K_A \approx 1.4$ and $K_S \approx 0.57$. The filling fraction is $\nu = 0.2$, hence the “Fermi wave vector” k_F is $\pi \times 0.2$. At momentum $2k_F$, both quantities develop cusps, indicating the presence of CDW order.

This shows that \mathcal{G}_{11} and $S(k)$ (Eq. 29) have the same Fourier transform of the density correlation function. If $S(k)$ develops cusps at $\pm 2k_F$, where $k_F = \pi\nu$ [23], when CDW order is present, we expect \mathcal{G}_{11} to have similar cusps at $k = k' \pm 2k_F$. In Fig. 5, we show one example of a quasi-supersolid (SS) state [21], where CDW order coexists with SF order. The parameters are listed in (e) of Table II. In the plot, the correlation function $C_{11}(q)$, an integration of $\mathcal{G}_{11}(k, k')$ along the direction $k = k'$ (Eq.

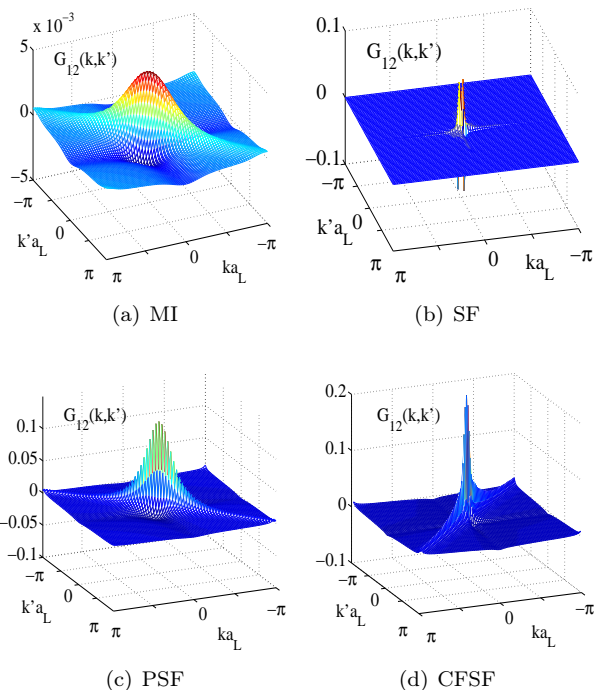


Figure 6: Noise correlations in the trapped system. The system size is 80 sites and $t/U = 0.02$. In (a), the system is in the SF state. The particle number of each species is 30, the trap frequency $8 \times 10^{-5}U$ and $U_{12}/U = 0.01$. In (b), the particle number of each species is 40, the trap frequency $1 \times 10^{-4}U$ and $U_{12}/U = -0.11$. The system has both MI and PSF orders. The MI state forms a plateau at unit-filling at the center of the trap and the PSF is formed at the edge. The PSF state at the edge causes the small peak along the $k = -k'$ direction, similar to the one in (c). However, this peak is at a much smaller amplitude than the one shown in (c), where the whole system is a PSF state. In (c), the particle number of each species is 20, the trap frequency $1 \times 10^{-5}U$ and $U_{12}/U = -0.11$. The whole system is in the PSF state. A strong pairing correlation is formed along $k = -k'$ direction. In (d), the particle number of each species is 30, the trap frequency is $8 \times 10^{-5}U$ and $U_{12}/U = 0.2$. The system has both CFSF and SF order. The CFSF order forms a plateau at half-filling at the center of the trap and the SF state towards the edges of the trap. The CFSF order causes a strong anti-pairing (particle-hole) correlation along $k = k'$ direction. At the same time, the SF order adds to the “dips” along $k = 0$ and $k' = 0$.

2), is compared with the structure factor $S(k)$ of the same state. In both functions, we can see cusps appearing at $\pm 2k_F$.

B. Noise correlations in the trapped system

We now discuss how the different types of order are affected by the presence of a trapping potential. To simulate the effect of a trap, we add a harmonic potential, $\Omega(j - j_c)^2(n_{1,j} + n_{2,j})$ to the Hubbard Hamiltonian in

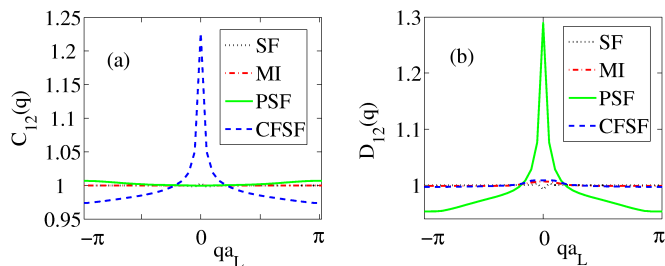


Figure 7: Correlations $C_{12}(q)$ and $D_{12}(q)$ for the states that are described in Fig. 7. In (a), we show the behavior of $C_{12}(q)$ (Eq. 2) in SF, MI, PSF and CFSF states. The strong anti-pairing (particle-hole) correlations in the CFSF state gives a strong signal around $q = 0$ in $C_{12}(q)$. This strong signal is also unique to the CFSF state and therefore can be used to detect to the CFSF order. In (b), we show the behavior of $D_{12}(q)$ (Eq. 3) in SF, MI, PSF and CFSF states. The strong pairing correlation in the PSF state is the reason for the high peak around $q = 0$ in $C_{12}(q)$. This suggests measuring $C_{12}(q)$ is a good way of detecting the PSF order.

Eq. 4, where j is the site index and j_c is the index at the center of the system. We then use the TEBD method to calculate the ground state. We also increase the system size to 80 lattice sites, and choose the total number of particles and the trap frequency to ensure that the boundary effect is negligible.

One interesting feature of a trapped system is that different orders can coexist in the trap. A well-known example is the MI plateau at the center of the trap surrounded by a SF at the edge [30]. For repulsive inter-species interaction, we find coexistence of a CFSF plateau with a SF at its edge and a MI plateau with PSF at the edges for attractive inter-species interactions [23]. Despite the potential complication of coexistence of orders, we find clear signals for the pairing correlations of the PSF phase and the anti-pairing correlations of the CFSF phase.

In Fig. 6, we show the behavior of $\mathcal{G}_{12}(k, k')$ in four different cases, where the orders at the center of the trap are SF, MI, PSF and CFSF respectively. We find that the general behavior of the noise correlation in a trap is very similar to its homogeneous counterpart. In Fig. 6 (c) and (d), \mathcal{G}_{12} shows clearly the feature of pairing correlations in the PSF state and the anti-pairing correlations in the CFSF state. In addition, we see some minor features attributed to the coexisting orders. In the case of CFSF in a trapped system, we can see the "dip" along $k = 0$ and $k' = 0$ because of the coexistence with the SF order. On the other hand, in the case of a MI in a trap, we can see pairing correlations as a result of the residual PSF state at the edges. This pairing signal is much smaller than when the whole system is in the PSF state.

To show that the peaks along $k = k'$ and $k = -k'$ in \mathcal{G}_{12} are detectable in experiments, we also calculate $C_{12}(q)$ (Eq. 2) and $D_{12}(q)$ (Eq. 3) for the four states. In the correlation $C_{12}(q)$ (Fig. 7 (a)), a high peak at $q = 0$ only appears in the case of the CFSF state. This

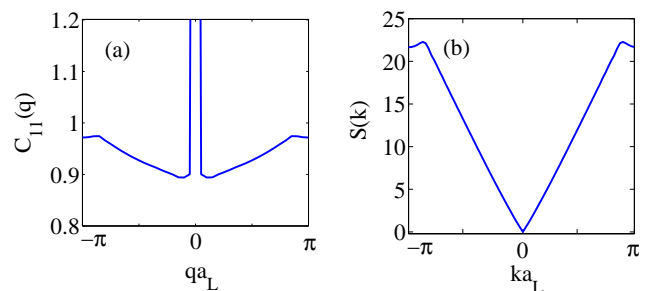


Figure 8: Noise correlation $C_{11}(q)$ and structure factor $S(k)$ in a PSF/CDW state. The system size is 80 sites and there are 20 particles of each species ($\nu = 0.25$). The trap frequency is $\Omega = 10^{-5}U$, the hopping $t = 0.02U$ and the inter-species interaction is $U_{12} = -0.11U$. The density at the center of the trap is roughly 0.45 per site and the cusps are developed around $\pm 0.9\pi$. The inhomogeneity of a trapped system means that the "Fermi wave vector" k_F is no longer $\pi\nu$, where ν is the average filling of the system. Instead, k_F can be evaluated as πn_{center} , where n_{center} is the density at the center of the trap,

peak corresponds to the peak in \mathcal{G}_{12} along $k = k'$ in the CFSF state and is a reflection of the anti-pair correlation in the CFSF state. Similarly, in $D_{12}(q)$, the high peak at $q = 0$ only appears in the PSF state, as a result of the strong pairing correlations in the PSF state. A similar measurement has been performed for fermionic mixtures to detect the pairing of fermions [2].

In addition to the PSF and CFSF order, we also look for the signal of CDW order in $\mathcal{G}_{11}(k, k')$ in the trapped system. In a trapped system, the CDW order is more difficult to establish especially in the PSF and SF states, because the varying local density makes the "Fermi wave vector" πn a spatially varying quantity. However, we can still see weakened cusps forming at the momentum roughly corresponding to $2\pi n_{center}$, where n_{center} is the density at the center of the trap. This may indicate that in the trapped system, the CDW order in PSF and SF states has a wave vector corresponding to the density at the center of the trap. For the CFSF state, because the system has a plateau at half filling, the wave vector $2k_F$ is π/a_L . Compared to the homogeneous case, this feature is slightly diminished due to the effect of the coexisting SF state in the trapped system. In Fig. 8, we show one case where CDW order coexists with PSF order in a trap. The system size is 80 sites and there are 20 particles of each species. The trap frequency $\Omega = 10^{-5}U$, $t = 0.02U$ and $U_{12} = -0.11U$. The density at the center of the trap is roughly 0.45 per site. The cusps are developed around $\pm 0.9\pi$, which is roughly $2\pi n_{center}$.

C. Determination of Luttinger parameters from experimental data

Another important question is whether we can use the noise correlation \mathcal{G}_{12} to measure the Luttinger parameters, K_S and K_A , in the PSF and CFSF regimes. The LL calculation shows that as the system size approaches infinity, the noise correlation \mathcal{G}_{12} approaches a power law decay with the power $-1/K_S$ in the PSF regime and with $-1/K_A$ in the CFSF regime (see Eqs. 21 and 22). In our numerical results for $C_{12}(q)$ and $D_{12}(q)$, we indeed find that the decay from the peak at $q = 0$ satisfies the algebraic decay. To find out the power of the algebraic decay, we fit the function $C_{12}(q)$ in the PSF regime and $D_{12}(q)$ in the CFSF regime with the fitting function,

$$F(q) = A|\sin(2q)|^{-1/K} + B, \quad (30)$$

where B is the minimum value of $C_{12}(q)$ or $D_{12}(q)$ and A and K are the fitting parameters. In the PSF case ($U_{12}/U = -0.11$), we find that K is 1.3 ± 0.1 . This is indeed very close to the value of K_S , which is estimated at 1.4 ± 0.1 obtained by the algebraic fit of R_S . In the CFSF case ($U_{12}/U = 0.2$), we find that K is roughly 1.48 ± 0.1 , while the value of K_A extracted from the algebraic fit of R_A is also at 1.48 ± 0.12 . Because of the singularity at $q = 0$, a reasonable values of K can be obtained by a simple algebraic decay function, $Aq^{-1/K} + B$, around small q . This shows that even in a trapped system, one can still assume a algebraical relationship predicted in the LL theory (Eqs. 21 and 22) and estimate the values of the Luttinger parameters by studying the power of the decay from the peak at $q = 0$.

V. CONCLUSIONS

We have studied the behavior of noise correlations for a binary bosonic mixture in optical lattices. We consider different regions of the phase diagram and we show that the noise correlations have different signatures for different phases. In particular, we discuss the measurement of the noise correlations as a means for detection of the paired superfluid (PSF) and counter-flow superfluid (CFSF) order. Our study of a harmonically trapped system shows that the inhomogeneity modifies the noise correlation, due to the coexistence of different orders within the trap. These modifications can be understood in terms of the results for the homogeneous system. What we find very encouraging is that even with the presence of a trap, the noise correlations still have distinctive features for each order, and the peak structure of the noise correlation \mathcal{G}_{12} in the PSF/CFSF regime still obeys the algebraic decay relationship predicted by the LL theory. This means that one can use the noise correlation to estimate the Luttinger parameters in these two regimes. All these results would be useful for experiments aimed at detecting the pairing and anti-pairing orders that can exist in ultracold atom systems.

Acknowledgments

We thank I. Danshita for useful discussions. This work was supported by the National Science Foundation under Physics Frontiers Center Grant PHY-0822671. L.M. acknowledges support from a NRC/NIST fellowship.

-
- [1] S. Fölling, F. Gerbier, A. Widera, O. Mandel, T. Gericke, and I. Bloch, *Nature* **434**, 481-484(2005).
 - [2] M. Greiner, C. A. Regal, J. T. Stewart, and D. S. Jin, *Phys. Rev. Lett.* **94**, 110401 (2005).
 - [3] I. B. Spielman, W. D. Phillips, and J. V. Porto, *Phys. Rev. Lett.* **98**, 080404 (2007).
 - [4] E. Altman, E. Demler, and M. D. Lukin, *Phys. Rev. A* **70**, 013603 (2004).
 - [5] L. Mathey, A. Vishwanath, and E. Altman, *Phys. Rev. A* **79**, 013609 (2009).
 - [6] L. Mathey, E. Altman, and A. Vishwanath, *Phys. Rev. Lett.* **100**, 240401 (2008).
 - [7] A. Imambekov, I. E. Mazets, D. S. Petrov, V. Gritsev, S. Manz, S. Hofferberth, T. Schumm, E. Demler, and J. Schmiedmayer, *Phys. Rev. A* **80**, 033604 (2009).
 - [8] V. W. Scarola, E. Demler, and S. Das Sarma, *Phys. Rev. A* **73**, 051601(R) (2006).
 - [9] A. Lüscher and A. M. Läuchli, *Phys. Rev. A* **76**, 043614 (2007); A. Lüscher, R. M. Noack, and A. M. Läuchli, *Phys. Rev. A* **78**, 013637 (2008).
 - [10] F. Schreck, L. Khaykovich, K. L. Corwin, G. Ferrari, T. Bourdel, J. Cubizolles, and C. Salomon, *Phys. Rev. Lett.* **87**, 080403 (2001).
 - [11] A. Görlitz, J. M. Vogels, A. E. Leanhardt, C. Raman, T. L. Gustavson, J. R. Abo-Shaeer, A. P. Chikkatur, S. Gupta, S. Inouye, T. Rosenband, and W. Ketterle, *Phys. Rev. Lett.* **87**, 130402 (2001).
 - [12] T. Kinoshita, T. Wenger, and D. S. Weiss, *Science* **305**, 1125 (2004).
 - [13] J.-B. Trebbia, J. Esteve, C. I. Westbrook, and I. Bouchoule, *Phys. Rev. Lett.* **97**, 250403 (2006).
 - [14] A. H. van Amerongen, J. J. P. van Es, P. Wicke, K. V. Kheruntsyan, and N. J. van Druten, *Phys. Rev. Lett.* **100**, 090402 (2008).
 - [15] I. Bouchoule, N. J. Van Druten, and C. I. Westbrook, e-print arXiv:0901.3303.
 - [16] B. Paredes, A. Widera, V. Murg, O. Mandel, S. Foelling, I. Cirac, G. Shlyapnikov, T. W. Hänsch and I. Bloch, *Nature* **429**, 277 (2004).
 - [17] T. Stöferle, H. Moritz, M. Köhl and T. Esslinger, *Phys. Rev. Lett.* **92**,130403(2004).
 - [18] A. Widera, S. Trotzky, P. Cheinet, S. Fölling, F. Gerbier, and I. Bloch, *Phys. Rev. Lett.* **100**, 140401 (2008).
 - [19] A. M. Rey, I. I Satija, and C. W Clark, *J. Phys. B* **39**,

- S177-S190 (2006); A. M. Rey, I. I. Satija, and C. W. Clark, *Phys. Rev. A* **73**, 063610 (2006).
- [20] A. Kuklov, N. Prokof'ev and B. Svistunov, *Phys. Rev. Lett.* **92**, 050402 (2004); *Phys. Rev. Lett.* **92**, 030403 (2003).
- [21] L. Mathey, I. Danshita and C. W. Clark, *Phys. Rev. A* **79**, 011602(R) (2009).
- [22] G. G. Batrouni, F. Hébert and R. T. Scalettar, *Phys. Rev. Lett.* **97**, 087209 (2006); V. W. Scarola and S. Das Sarma, *ibid.* **95**, 033003 (2005); P. Sengupta, L. P. Pryadko, F. Alet, M. Troyer and G. Schmid, *ibid.* **94**, 207202 (2005); S. Wessel and M. Troyer, *ibid.* **95**, 127205 (2005); D. Heidarian and K. Damle, *ibid.* **95**, 127206 (2005); R. G. Melko, A. Paramekanti, A. A. Burkov, A. Vishwanath, D. N. Sheng, and L. Balents, *ibid.* **95**, 127207 (2005); H.P. Büchler and G. Blatter, *ibid.* **91**, 130404 (2004); M. Boninsegni and N. Prokof'ev, *ibid.* **95**, 237204 (2005); M. Boninsegni, *J. Low. Temp. Phys.* **132**, 39 (2005); P. P. Orth, D. L. Bergman and K. Le Hur, *Phys. Rev. A* **80**, 023524 (2009); D. L. Kovrizhin, G. Venketeswara Pai and S. Sinha, *Euro. Phys. Lett.* **72**, 162 (2005); F. Karim Pour, M. Rigol, S. Wessel, and A. Muramatsu, *Phys. Rev. B* **75**, 161104 (2007). C. Trefzger, C. Menotti, M. Lewenstein, *Phys. Rev. Lett.* **103**, 035304 (2009)
- [23] A. Hu, L. Mathey, I. Danshita, E. Tiesinga, C. J. Williams, and C. W. Clark, *Phys. Rev. A* **80**, 023619 (2009).
- [24] C. Menotti and S. Stringari, arXiv:0912.4452.
- [25] G. Vidal, *Phys. Rev. Lett.* **98**, 070201 (2007); G. Vidal, *ibid.* **91**, 147902 (2003); *ibid.* **93**, 040502 (2004); S. R. White and A. E. Feiguin, *ibid.* **93**, 076401 (2004); I. Danshita and P. Naidon, *Phys. Rev. A* **79**, 043601 (2009); I. Danshita and C. W. Clark, *Phys. Rev. Lett.* **102**, 030407 (2009); L. D. Carr, M. L. Wall, D. G. Schirmer, R. C. Brown, J. E. Williams, and Charles W. Clark, *Phys. Rev. A* **81**, 013613 (2010);
- [26] D. Jaksch, C. Bruder, J. I. Cirac, C. W. Gardiner, and P. Zoller, *Phys. Rev. Lett.* **81**, 3108 (1998).
- [27] F. D. M. Haldane, *Phys. Rev. Lett.* **47**, 1840 (1981).
- [28] M. A. Cazalilla, *J. Phys. B: At. Mol. Opt. Phys.* **37**, S1 (2004).
- [29] T. Giamarchi, *Quantum physics in one dimension*, (Oxford Univ. Press, Oxford, UK, 2004).
- [30] S. Fölling, A. Widera, T. Müller, F. Gerbier, and I. Bloch, *Phys. Rev. Lett.* **97**, 060403 (2006).